

Ship observations coasting South America in the tropical Pacific Ocean

S. P. de Szoeke*, C. W. Fairall, and Sergio Pezoa

NOAA/ESRL Physical Sciences Division, Boulder, Colorado, USA.

*NOAA/ESRL/Physical Sciences Division 325 Broadway, R/PSD3, Boulder, CO. 80305, USA. *e-mail*:Simon.deSzoeke@noaa.gov.

Abstract

In October 2007 the NOAA ship *Ronald H. Brown* sailed to the south within 300 km of the coast of Ecuador and Peru, sampling surface meteorology, air-sea turbulent and radiative fluxes, cloud properties, and upper-air soundings from the equator to 20° S. Two distinct water masses characterize the coastal region: cold pool water below 19° C in the southern hemisphere, and warm pool water above 20° C to the north, with a transition between the water masses at 2.5° S. Net turbulent and radiative fluxes warm the cool water south of 2.5° S by 100 W m⁻², but do not warm the equatorial water significantly. Winds blow parallel to the shore, about 5 m s⁻¹ over the cold pool and 7 m s⁻¹ over the equator. Stratocumulus clouds are remarkably solid over the coastal cold pool, with only brief periods of partial clearing, mostly in the afternoon. Lower aerosol concentrations and thicker clouds observed farther from the coast on 22-23 October may be evidence of the ship encountering a pocket of open cells. Data from this cruise and other NOAA Stratus cruises (2001 and 2003-2007) are publicly available and may be used for model studies or for future field experiments.

1. Introduction

The temperature of the tropical Pacific Ocean at the coastal boundary is determined by a complex balance of upwelling, surface fluxes, and transport; which in turn depend on the wind and solar forcing at ocean surface. Southeasterly winds blow parallel to the coast in the southern hemisphere, causing offshore Ekman transport and coastal upwelling that cools the ocean surface. Coastal sea surface temperature (SST) propagates westward by Bjerknes (1969) and wind-evaporation-SST feedback (reviewed by Xie 2004), and is amplified by the high albedo of stratus clouds that form in the marine atmospheric boundary layer (MABL). Thus coastal SST is important for the whole ocean, and cool SST at the southern coast sets the meridional asymmetry of heating and the Hadley Cell in the Pacific Ocean, with consequences for the seasonal cycle and migration of the intertropical convergence zone (ITCZ) (Xie 1994, de Szoeke and Xie 2008).

Because of the shallow MABL, steep Andean mountains, and coupled cloud, aerosol, and ocean interactions, simulating stratiform clouds and surface winds has been challenging for coupled general circulation models (Ma et al. 1996, Gordon et al. 2000). These interactions are the focus of the planned VAMOS Ocean Cloud Atmosphere Land Study (VOCALS) regional experiment planned for autumn 2008. Already Stratus cruises undertaken jointly by NOAA and Woods Hole Oceanographic Institution (WHOI) in autumn of 2001 and 2003-2007 have ventured into the southeastern tropical Pacific to quantify the ocean, MABL, and cloud dynamics responsible for the near-surface heat budget. In collaboration with Ecuadorian and Peruvian scientists and their governments, the Stratus cruise in October 2007 made a unique transect along the coast of South America, from the Equator to 20° within 300 km of shore. The track of the ship on this transect is shown by the dashed line following the coast at right in Fig. 1. Each red dash is a six hour interval, and numbers along the track indicate the date of October, Universal Time (UT). The ship traveled into the wind from north to south.

2. Instruments and sampling

Three sets of instruments on the NOAA ship *Ronald H. Brown* (*RHB*) made measurements during the 2007 Stratus cruise (Fairall et al. 2003, Fairall and Bradely 2006): NOAA PSD near surface meteorology, cloud remote sensing and aerosol number sampling from the ship, and upper-air soundings.

The NOAA/ESRL Physical Sciences Division (PSD) Weather and Climate Physics Branch (formerly ETL) has outfitted the *RHB* with a mobile set of accurate and fast sensors which acquire observations of the near-surface atmosphere with an accuracy suitable to compute air-sea fluxes (Fairall et al. 2003). Instruments on a jackstaff at the bow of the ship sample air temperature, humidity, wind, and ship motion. Sea surface temperature is measured by a floating “sea snake” thermometer at approximately 5 cm depth. At this depth the thermometer samples the daylight warm layer, but not the cool skin layer. The optical rain gauge malfunctioned and was switched off during Stratus 2007.

Direct surface turbulent fluxes of momentum and heat are computed by covariances of high-rate (20 Hz) temperature and velocity components from a sonic anemometer-thermometer. Humidity fluxes are calculated with observations of water vapor from a 3-band infrared Licor 7500 optical absorption instrument. The 2007 Stratus cruise pioneered the use of multiple Licor instruments, with the goal of developing a reliable autonomous shipboard system with enough precision to measure CO₂ fluxes directly.

Turbulent fluxes displayed here are computed from bulk quantities by the Fairall et al. (2003) algorithm. Downward solar and infrared radiation are measured by a pyranometer and a pyrgeometer, respectively. Surface meteorology and fluxes were averaged to standard 5-minute time intervals beginning on the hour.

PSD uses an upward looking Radiometrics “mailbox” 24- and 31-MHz channel passive microwave radiometer to estimate column water vapor and liquid water (Hare et al. 2005, Fairall et al. 2008). A Vaisala 905-nm lidar ceilometer estimates cloudiness and up to 3 cloud base heights. An active 915-MHz NOAA radar wind profiler was operated with its antenna pointed vertically. Tur-

bulence and gradients of temperature and humidity at the MABL inversion scatter the radar pulse, from which we diagnose the height of the boundary layer to the nearest 60 m range gate. Valid returns from these three sensors are averaged to standard 5-minute intervals.

Vaisala global positioning system (GPS) digital rawinsondes were released into the atmosphere from the fantail of the ship approximately every 6 hours during the coastal transect from October 18-23. The rawinsonde release times and locations are indicated by open circles along the ship track in Fig. 1. Rawinsondes measured and telemetered temperature, relative humidity, pressure, and GPS position. Profiles of temperature, humidity, and winds with height are calculated and averaged to standard 10-m altitudes.

3. Surface meteorology

Arrows originating from the dashed ship track in Fig. 1 are centered 6-hour averages of the surface wind. The wind was extremely constant within each 6-hour period, with speed standard deviation less than or equal to 1 m s^{-1} . The wind speed $\| \mathbf{u} \|$ (black dashed line) is on average 5.6 m s^{-1} , with a 0.4 m s^{-1} offshore component. The wind follows the contour of the coast with a standard deviation in direction of under 20° in each 6 hour period. South of 12° S winds are as much as 40° degrees offshore of parallel to the local coast, reflecting the heading of the coast upstream of the ship between Paracas Peninsula and Arica.

The SST (red) and air temperature (blue) are plotted to the left of the ship track in Fig. 1. SST reaches a minimum of 15.5° C at 14° S and a maximum of 26.6° C at 2° N . Air temperature follows SST. The sea-air temperature difference is about 1.3° C south of 3° S , with diurnal variations of the same magnitude. On the nights of October 18, 19, and 21 local the SST cooled off to equal the air temperature, occasionally resulting in sensible heat flux from the air to the ocean. The air temperature is considerably cooler than the SST (3.5° C) in the warm pool north of 3° S , because advection from the south cools the surface air by $\sim 10^\circ \text{ C day}^{-1}$. The largest sea-air temperature difference of 4.25° C was observed in the afternoon downstream of the strong gradient at 2.5° S .

At right in Fig. 1 is the profile of air-sea heat fluxes along the track. Positive (rightward) fluxes represent heat leaving the ocean. The red curves are solar (R_s) and infrared (R_i) fluxes. The solar flux is plotted on a scale one tenth of the scale of the other fluxes, and its pulses indicate the time of local daylight. The black curves are latent and sensible turbulent heat fluxes. Latent heat flux E is in the neighborhood of $100\text{--}150\text{ W m}^{-2}$ north of 2.5° S , and about 50 W m^{-2} south of 2.5° S . Sensible heat flux H is about 30 and 10 W m^{-2} north and south of 2.5° S . Though solar flux has large diurnal variations, it does not appear to be noticeably different on either side of 2.5° S . The variability of the infrared flux increases south of 2.5° S , probably because the atmosphere has less water vapor and downward thermal radiation is more strongly modulated by clouds. Table 1 shows a mean heat budget of the upper ocean, averaging the whole coastal ship track, the part north of 2.5° S , and the part south of 2.5° S . To avoid diurnal sampling biases, we use the solar radiation averaged over the whole coastal leg for all of the budgets. The average solar radiation for the partial legs is nevertheless indicated in parentheses. In the warm pool to the north, the ocean surface is not losing or gaining heat within measurement error. Yet on the southern part of the leg, the cool ocean is warmed by a net 100 W m^{-2} .

4. Clouds and upper-air soundings

Rawinsondes were launched from the ship every 6 hours beginning October 18, 18:00 UT, and every 4 hours on October 23, providing snapshots of the vertical temperature and humidity structure of the atmosphere. All the soundings on the coastal leg are compiled in a time-height section of potential temperature θ and specific humidity q from 0-2.5 km altitude in Fig. 2a and b. Both quantities clearly show the trade-MABL inversion after October 20, with a well-mixed layer of high humidity ($7\text{--}8\text{ g kg}^{-1}$) and low potential temperature (287 K). By visual inspection we picked the 4 g kg^{-1} specific humidity (black) and 296 K (green) potential temperature contours to mark the boundary layer inversion. These contours follow the strong gradient at the MABL inversion south of 8° S , but the inversion is hard to diagnose north of 8° S . Before October 20, the

ship was under a convective weather system, with tall cumulus towers reaching far into the free troposphere. The strong humidity signal of these clouds was recorded by the soundings. The 4 g kg^{-1} contour rises more than a kilometer into the free troposphere and the stratification of the inversion and free troposphere are reduced during this stormy period. The atmosphere remained convectively disturbed above 1 km all the way to 8° S , beyond the southern extent (2.5° S) of warm-pool SST over 20° C .

Apart from the convective period, marine atmospheric boundary layer stratocumulus clouds were quite uniform in height and thickness. We diagnose cloud top from the soundings, and compared them with other estimates from independent ship observations in Fig. 2a. (The estimates are repeated in Fig. 2b for comparison to the humidity profile.) The crosses show the height of the minimum temperature in the sounding, assumed to be the base of the inversion. While the temperature minimum is associated with the cloud top, it is on-average 100 m below the level of the inversion indicated by strong gradients of humidity and potential temperature. The NOAA radar wind profiler receives strong signals scattered back from the gradients and turbulence at the inversion. Magenta dots show the height of maximum signal to noise ratio of the wind profiler radar returns. The wind profiler inversion height agrees well with the inversion found from the gradient in the soundings. These estimates of the inversion height agree with the level where LCL parcels would evaporate completely when mixed with 25-50% of environmental air (not shown).

The stratocumulus cloud base height observed by the laser ceilometer is plotted in green in Fig. 2a and b. The ceilometer cloud base is sometimes $\sim 100 \text{ m}$ higher than the LCL of a surface parcel (red), which indicates that dry air entrained from the free troposphere dilutes the water vapor in the cloud. The consistency of cloud base height from the ceilometer and the LCL, and the inversion height from the profiler and the temperature and humidity structure from the soundings gives us confidence in the accuracy of our measurements of cloud vertical structure.

The red line in Fig. 2c shows the integrated water vapor from the microwave radiometer. Integrated water vapor follows the surface humidity (Fig. 1), as most of the water vapor is trapped in the boundary layer.

The clouds are usually solid, with cloud fraction (green, Fig. 2c) rarely deviating from unity. An exception is the clear sky observed in on the first half of 19 October (UT), when the atmosphere is convective. Though partial clearing is observed on occasion, clear skies are only briefly observed in the stratocumulus region starting on the afternoons of 21-23 October (local).

The concentration of aerosol particles between 0.1 and 5 μm is highest late on 18 October when the ship passes closest to land offshore of Cabo San Lorenzo. The aerosol concentration dips below 100 cm^{-3} on October 22, with a minimum of 25 cm^{-3} on 23 October. Displacement of the ship further from shore on 22 October, after it had rounded Paracas Peninsula, could be responsible for the lower aerosol concentrations. Though clear skies were only observed briefly during these afternoons of lower aerosol concentration, the dip in aerosol concentration was similar to that in pockets of open cells (POCs) (Stevens et al. 2005) observed during the remainder of the 2007 Stratus cruise.

The clearing seen from the ship in the early afternoon (local) of 22 October was associated with a thickening of the clouds, as seen from the ceilometer and the LCL in Fig. 2. Clouds remain thicker during the time of low aerosol concentrations. Satellite imagery from the NOAA-17 polar-orbiting satellite taken on 22 October, 14:25 UT (Fig. 3) shows two clear regions on either side of the ship (marked in its position at the time of the image at 18.6° S, 75.4° W). The clear region adjoining the coast is most likely due to the boundary layer being too shallow for parcels to reach their LCL. The clear region neighboring ship to its southwest is one of several pockets of open cells visible at this time. At the time of the image, the ship is barely outside the POC, but is headed toward its wider end. Though Fig. 3 is the only image from 22 October, on other days POCs were seen to expand during the afternoon.

5. Summary

In October 2008 the NOAA ship *Ronald H. Brown* followed the tropical Pacific coastline of western South America from the equator to 20° S. Surface ocean and meteorological measurements

discern warm water near and displaced south of the equator and a cooler water mass south of 2.5° S. Winds blew parallel to the coast and were steady in speed and direction. Net heat gained by the surface of the ocean was 100 W m^{-2} over the cool coastal water, and not significantly different from zero over the warmer equatorial water.

Observations from multiple sensors were mutually consistent about the height of cloud bases and tops, and consistent with parcel and mixing-line computations of cloud vertical structure. Stratocumulus clouds were solid, with brief episodes of partial clearing, mostly in the afternoons. Lower aerosol concentrations and slightly thicker clouds were observed 22-23 October when the ship encountered a pocket of open cells.

The data presented here are part of an integrated data set available at <http://www.esrl.noaa.gov/psd/people/Simon.deSzoeko/synthesis.html>. Sounding and *in situ* time series data are available for the Stratus cruises of 2001 and 2003-2007. These data are suitable for verifying climatology, variability, and feedbacks in reanalysis and model products of the eastern tropical Pacific region. The various legs of these cruises also provide context for the VAMOS Ocean Cloud Atmosphere Land Study (VOCALS) Regional Experiment in autumn 2008.

Acknowledgments.

This work has been funded by the support of a National Research Council fellowship, and by the United States National Oceanic and Atmospheric Administration. We also acknowledge the crew and scientific party of the *RHB*, especially LiSan Yu, Sean Whelan, and Chief Scientist Robert Weller. Dan Wolfe and Ludovic Bariteau of PSD have contributed to the installation and maintenance of the NOAA sensors and data acquisition systems on the ship.

REFERENCES

- Bjerknes, J., 1969: Atmospheric teleconnections from the equatorial Pacific. *Monthly Weather Review*, **97**, 163–172.
- de Szoeke, S. P. and S.-P. Xie, 2008: The tropical eastern Pacific seasonal cycle: Assessment of errors and mechanisms in IPCC AR4 coupled ocean-atmosphere general circulation models. *Journal of Climate*, in press.
- Fairall, C. and E. F. Bradley, 2006: A guide to making climate quality meteorological and flux measurements at sea. NOAA Technical Memorandum OAR PSD-311, NOAA Earth System Research Laboratory, Physical Sciences Division.
- Fairall, C. W., E. F. Bradley, J. E. Hare, A. A. Grachev, and J. B. Edson, 2003: Bulk parameterization of air-sea fluxes: updates and verification for the coare algorithm. *Journal of Climate*, **19** (4), 571–591.
- Fairall, C. W., T. Uttal, D. Hazen, J. Hare, M. F. Cronin, N. A. Bond, and D. E. Veron, 2008: Cloud, radiation, and surface forcing in the equatorial eastern Pacific. *Journal of Climate*, in press.
- Gordon, C. T., A. Rosati, and R. Gudgel, 2000: Tropical sensitivity of a coupled model to specified ISCCP low clouds. *Journal of Climate*, **13** (13), 2239–2260.
- Hare, J., C. Fairall, T. Uttal, D. Hazen, M. F. Cronin, N. Bond, and D. Veron, 2005: Cloud, radiation, and surface forcing in the equatorial eastern Pacific. NOAA Technical Memorandum OAR PSD-307, NOAA Earth System Research Laboratory, Physical Sciences Division.
- Ma, C.-C., C. R. Mechoso, A. W. Robertson, and A. Arakawa, 1996: Peruvian stratus clouds and the tropical Pacific circulation: a coupled ocean-atmosphere GCM study. *Journal of Climate*, **9**, 1635–1645.

Stevens, B., G. Vali, K. Comstock, R. Wood, M. C. V. Zanten, P. H. Austin, C. S. Bretherton, and D. H. Lenschow, 2005: Pockets of open cells and drizzle in marine stratocumulus. *Bulletin of the American Meteorological Society*, **86** (1), 51–57.

Xie, S.-P., 1994: On the genesis of the equatorial annual cycle. *Journal of Climate*, **7** (12), 2008–2013.

Xie, S.-P., 2004: The shape of continents, air-sea interaction, and the rising branch of the Hadley circulation. *The Hadley Circulation: Past, Present and Future*, H. F. Diaz and R. S. Bradley, Eds., Kluwer Academic Publishers.

List of Figures

- 1 Track of the *RHB* along the coast of South America on the 2007 Stratus cruise. Dashed red lines indicate 6-hour intervals; October days 18-24 are printed at right. 6-hour average observed surface wind vectors (blue) point from the ship track. Curves from right to left of ship track: Sea surface temperature (T_s , red), 18 m air temperature (T_a , blue) and humidity (q , green), surface turbulent latent and sensible (H and E , black), and net radiative solar and infrared long wave (R_s and R_i , red) fluxes. 12
- 2 Profiles of 0-2.5 km altitude lower tropospheric (a) potential temperature and (b) specific humidity from rawinsondes. Panel (c) shows hundreds of aerosol particles per cm^3 (blue), column-integrated water vapor (cm, red), and cloud fraction (green). In panels (a) and (b) the crosses denote the height of minimum temperature at the base of the inversion. The green and black solid lines indicate the 296 K and 4 g kg^{-1} contours from the soundings, respectively. Small green dots are the cloud base determined by the laser ceilometer, and magenta dots are the MABL inversion from the radar wind profiler. The red line is the lifting condensation level of a surface parcel. The horizontal coordinate is time, and the latitude of observation is printed along the top of each axis. 13
- 3 Visible radiance from the NOAA-17 polar-orbiting satellite on October 22 at 14:25 UT. At the time of the image, the ship was at the position marked (18.6° S , 75.4° W) between the clear boundary layer neighboring the coast and the pocket of open cells to the southwest. 14

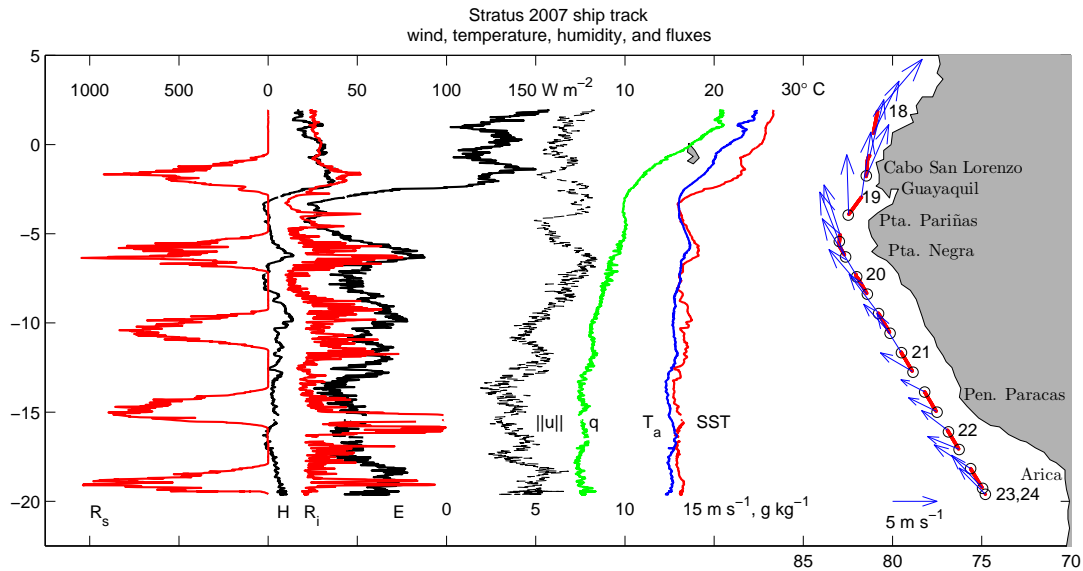


FIG. 1. Track of the *RHB* along the coast of South America on the 2007 Stratus cruise. Dashed red lines indicate 6-hour intervals; October days 18-24 are printed at right. 6-hour average observed surface wind vectors (blue) point from the ship track. Curves from right to left of ship track: Sea surface temperature (T_s , red), 18 m air temperature (T_a , blue) and humidity (q , green), surface turbulent latent and sensible (H and E , black), and net radiative solar and infrared long wave (R_s and R_i , red) fluxes.

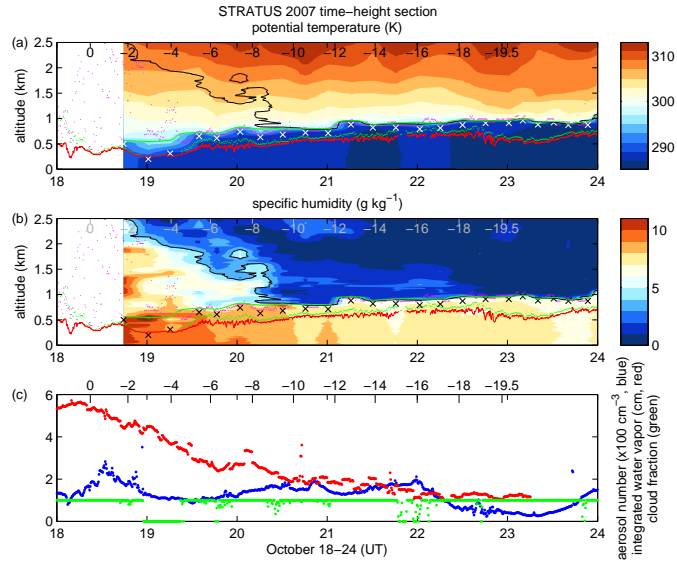


FIG. 2. Profiles of 0-2.5 km altitude lower tropospheric (a) potential temperature and (b) specific humidity from rawinsondes. Panel (c) shows hundreds of aerosol particles per cm³ (blue), column-integrated water vapor (cm, red), and cloud fraction (green). In panels (a) and (b) the crosses denote the height of minimum temperature at the base of the inversion. The green and black solid lines indicate the 296 K and 4 g kg⁻¹ contours from the soundings, respectively. Small green dots are the cloud base determined by the laser ceilometer, and magenta dots are the MABL inversion from the radar wind profiler. The red line is the lifting condensation level of a surface parcel. The horizontal coordinate is time, and the latitude of observation is printed along the top of each axis.

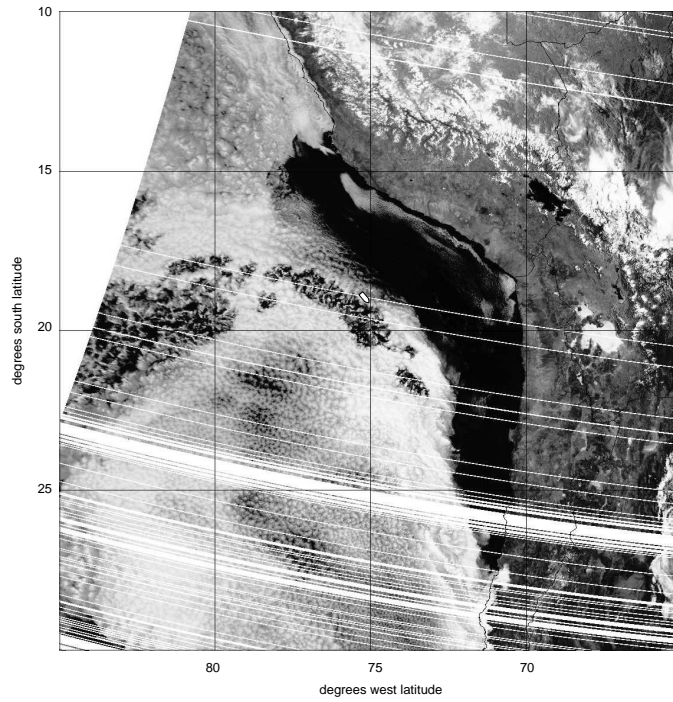


FIG. 3. Visible radiance from the NOAA-17 polar-orbiting satellite on October 22 at 14:25 UT. At the time of the image, the ship was at the position marked (18.6° S, 75.4° W) between the clear boundary layer neighboring the coast and the pocket of open cells to the southwest.

List of Tables

1	Heat flux components (W m^{-2}) into the ocean for the coastal transect, north of 2.5° S , and south of 2.5° S	16
---	---	----

TABLE 1. Heat flux components (W m^{-2}) into the ocean for the coastal transect, north of 2.5° S , and south of 2.5° S .

	whole track	latitude $>2.5^\circ \text{ S}$	latitude $<2.5^\circ \text{ S}$
solar	188	(147)	(198)
IR	-30	-30	-30
sensible	-8	-27	-4
latent	-66	-125	-52
total	82	6	102